Long range ordering in self-assembled Ni arrays on patterned Si

D.C. Gonzalez[a],*, M.E. Kiziroglou[a], X. Li[a], A.A. Zhukov[b], H. Fangohr[d],
P.A.J. de Groot[b], P.N. Barttlet[c], C.H. de Groot[a]

[a]*Nanoscale Systems Integration Group, School of Electronics and Computer Science, University of Southampton, Southampton SO17 1BJ, UK*
[b]*School of Physics and Astronomy, University of Southampton, Southampton SO17 1BJ, UK*
[c]*School of Chemistry, University of Southampton, Southampton SO17 1BJ, UK*
[d]*School of Engineering Sciences, University of Southampton, Southampton SO17 1BJ, UK*

Available online 25 February 2007

Abstract

We have succeeded in aligning self-assembled structures by using a lithographically defined stripe. The 140 nm wide by 100 nm high SiO$_2$ strip is shown to guide the assembly of 500 nm latex spheres so that spheres are aligned along the strip and are in registration on either side of the strip. This method can be used to increase long-range ordering in magnetic storage systems without compromising the density. Inverse sphere Ni arrays were made by electrodeposition through the latex template. We also show that the hexagonal symmetry of the resulting inverse sphere Ni arrays can be simulated using the approach presented below.
© 2007 Elsevier B.V. All rights reserved.

1. Introduction

Self-assembly is defined as the autonomous organisation of components into patterns or structures without human intervention [1]. Self-assembly is nowadays regarded as an alternative to overcome limitations found in both conventional and e-beam lithographic methods for transferring patterns. This makes self-assembly very promising because it could be used in patterned storage media to increase the storage densities currently available on hard disks up to an estimated density of 1 Tbit/in^2 [2]. Advances in the use of various methods for self-assembly have been made [3–9]. However, orientation and long-range ordering of the self-assembled template remains a problem. It has been shown that by defining tracks on the substrate, the self-assembly can be controlled to a certain extent [10,11]. But this still does not address the long-range ordering required for magnetic storage. In this study, we will show that long-range ordering in self-assembled structures can be achieved by the guidance of a lithographically defined stripe. Our

self-assembly method is based on latex spheres which are used as a template for the electrodeposition of Ni. It has been shown by various groups that the self-assembled spheres can be used as an etch template to create pillars and other structures useful for magnetic storage [12,13]. To study the properties of the template, we used latex spheres as a direct template for electrodeposition. This creates so-called antidote or inverse sphere arrays of Ni. In a previous paper, we have shown the hexagonal symmetry of the coercivity in these structures [14]. Here we will show that the observed symmetry can be explained qualitatively by the micromagnetic simulation of only one small section of the patterned film.

2. Experimental

Fig. 1 illustrates the steps followed to fabricate the inverse sphere Ni array analysed in this study. N-type ⟨100⟩ single-side polished silicon wafers with resistivity 0.01–0.02 Ω cm were used as substrates. Then a 250 nm thick layer of SiO$_2$ was thermally grown on the polished side. The guiding stripes were defined by conventional

*Corresponding author. Tel.: +44 23 8059 7389; fax: +44 23 8059 3029.
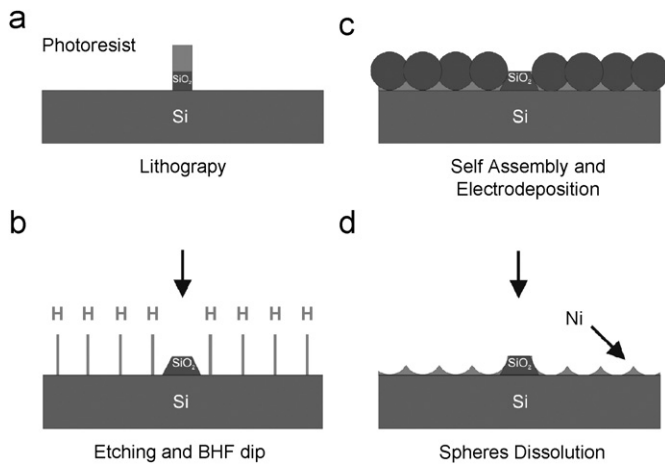E-mail address: dcg04r@ecs.soton.ac.uk (D.C. Gonzalez).

Fig. 1. Process flow for guided self-assembly of inverse sphere magnetic arrays. The width of the resulting guiding stripe is 140 nm.

Fig. 2. SEM micrograph of a Ni inverse sphere array, guided by a 140 nm wide and 100 nm high SiO_2 stripe. In the inset, the mechanism of lining up the arrays at either sides of the stripe is demonstrated.

lithography (Fig. 1a). Wet etch was used to eliminate the excess of SiO_2 and leave only the guiding stripes. A 20:1 BHF dip was used to leave the Si surface H-terminated and hence, hydrophobic (Fig. 1b). Shortly after this BHF dip, 500 nm diameter latex spheres were self-assembled on the substrates by slow evaporation of a colloidal water suspension containing 1 wt% of latex spheres. Electrodeposition was used to grow inverse sphere Ni arrays directly on Si without a back contact (Fig. 1c). Another 20:1 BHF dip was carried out just before electrodeposition in order to remove the native oxide and leave the Si surface H-terminated. The conditions used during electrodeposition can be found elsewhere [15]. Finally, the latex spheres dissolution was performed with tetrahydrofuran (C_4H_8O), which resulted in the inverse sphere Ni arrays on Si studied below (Fig. 1d). Characterisation was carried out using scanning electron microscopy (SEM). Magnetic measurements were carried out in a magneto-optical Kerr effect (MOKE) rig. Measurements have been performed at room temperature.

3. Results and discussion

A self-assembled Ni inverse sphere array guided by a 140 nm wide and 100 nm thick SiO_2 stripe is presented in Fig. 2. It can be noticed that the array is free of fractures and it follows the orientation of the guiding stripe. Moreover, the phases of the array on either side of the stripe are aligned. This is accomplished by continuation of the sphere self-assembly over the stripe, lining up the two sides, as illustrated in the inset in Fig. 2. The self-assembly is hence not hampered by the lithographically defined guidance stripe, while at the same time it forces the orientation of the self-assembly creating therefore longer-range ordering. Although some defects on the anti-sphere array caused by missing spheres can also be observed, this result is particularly important for patterned storage media as it reveals that long-range self-assembly can be achieved by lining-up a series of guided self-assembled magnetic
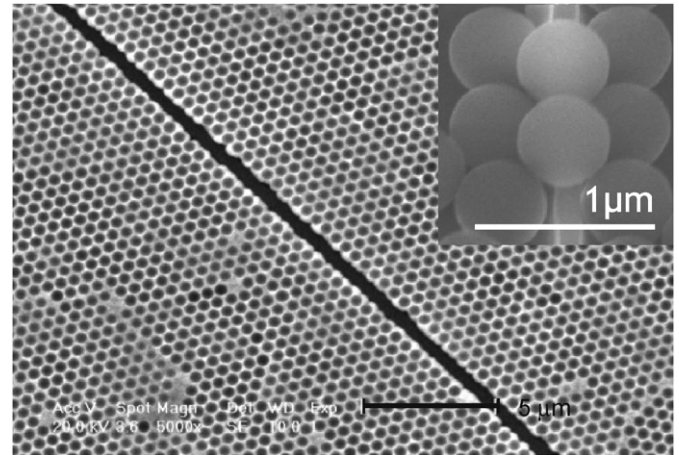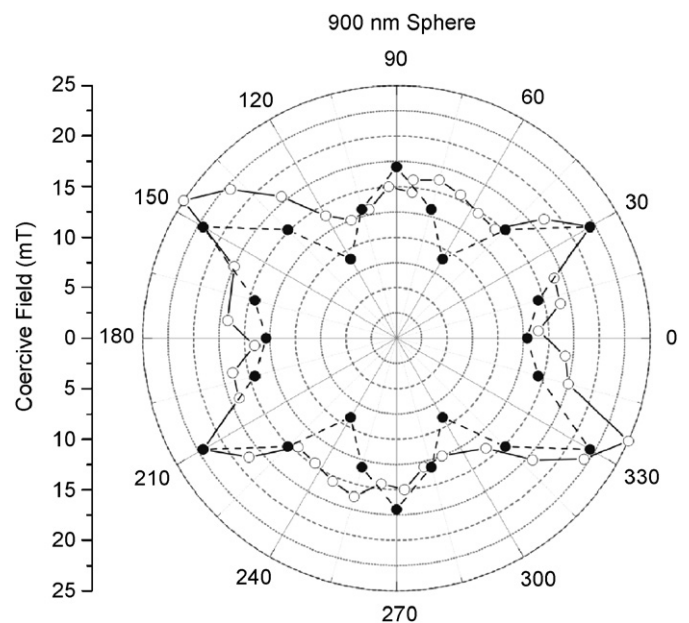

Fig. 3. Comparison of coercivities between experimental and simulated data showing angle dependence of coercivity. Open circles correspond to MOKE measurements. Filled circles correspond to simulation data taking uniaxial magnetocrystalline anisotropy into account. Simulation results were divided by 2 to normalise them with the experimental data and it can be seen that simulations reproduce the qualitative behaviour of the experimental data.

arrays. Due to the fact that the guiding stripe width is about the same order or smaller than the spheres themselves, storage density will not be greatly compromised.

MOKE measurements were carried out in an inverse sphere Ni array prepared using 900 nm latex spheres. The coercivities measured when the magnetic fields were applied at various angles are shown in Fig. 3. From this figure it can be readily noticed the dependence of the coercivity on the direction of the magnetic field. It can also be noticed the six-fold symmetry corresponding to the hexagonal configuration of the nanostructured array.
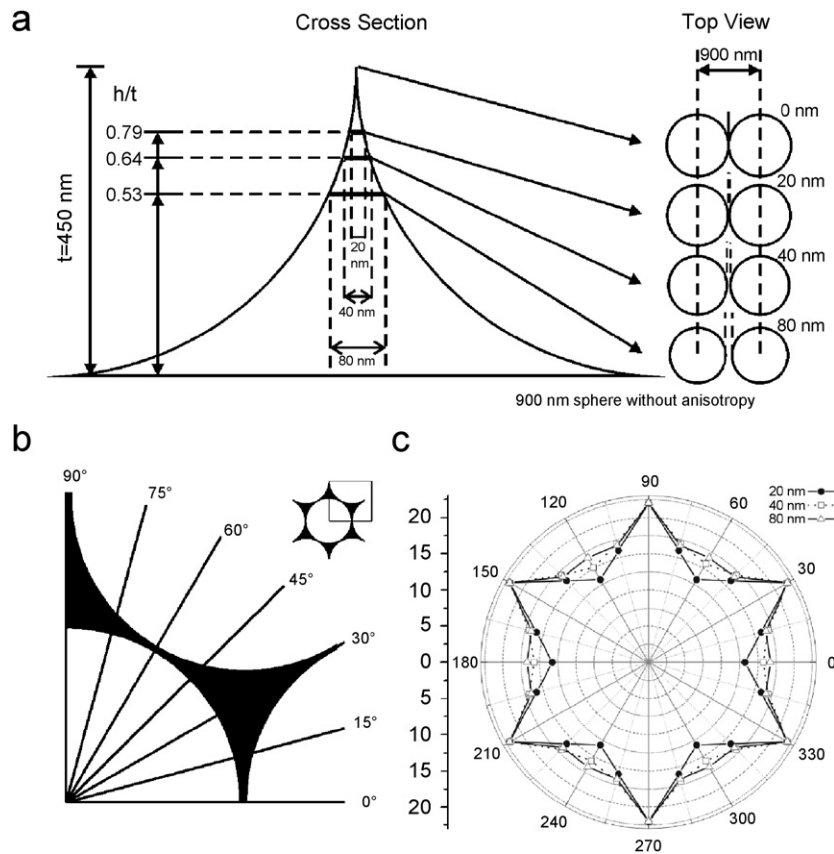
Fig. 4. Schematic explanation of our single-cylinder approach to explain six-fold symmetry of coercivitiy found in MOKE measurements. Part (c) shows that at lower cross section heights the anisotropy induced by the patterning becomes smaller.

Micromagnetic simulations using OOMMF [16] were carried out in order to explain the behaviour of the measurements presented above. The cylinders considered were 20 nm height with a diameter of 880 nm. This diameter corresponds to the section of the film where the distance between spheres is approximately 20 nm as shown in Fig. 4(a). The simulated model consisted of a two-dimensional system formed by a single cylinder surrounded by its six closest neighbours as shown in the inset in Fig. 4(b). A finite difference grid was applied to this system with cells having dimensions of size 5 nm × 5 nm. The height of the cells was 20 nm corresponding to the cylinder height mentioned above. The parameters of the material correspond to those of Ni [17] ($M_s = 4.9 \times 10^5$ A/m, $A = 9 \times 10^{-12}$ J/m). A value of $K_1 = -5.6$k J/m^3 was used for simulations considering a uniaxial magnetocrystalline anisotropy. Simulations consisted of the calculation of the magnetisation reversal processes taking place when the magnetic fields are applied at different angles. Due to the hexagonal structure of the array, the obtained coercivities from reversal processes at the angles displayed in Fig. 4(b) can be extrapolated and compared with the experimental measurements as shown in Fig. 3. All coercivity values from our simulations were divided by 2 in order to normalise them with the experimental data. The observed discrepancy is mainly due to the fact that the simulations

were carried out for a single anti-sphere and not for the whole array. Nonetheless, Fig. 3 shows that our single-cylinder approach reproduces qualitatively the anisotropy produced by the nanostructuring and suggests that shape anisotropy plays a significant role in the magnetisation reversal.

4. Conclusion

We have succeeded in aligning self-assembled structures by using a lithographically defined stripe. This method can be used to increase long-range ordering in magnetic storage systems without compromising the density. We have also shown that the hexagonal symmetry of the resulting inverse sphere Ni arrays can be simulated using the approach presented above.

References

[1] G.M. Whitesides, B. Grzybowski, Science 295 (2002) 2418.
[2] S. Sun, C.B. Weller, D. Folks, L. Moser, Science 287 (2000) 1989.
[3] J.C. Hulteen, C.R. Martin, J. Mater. Chem. 7 (1997) 1075.
[4] T. Thurn-Albrecht, J. Schotter, G.A. Kastle, N. Emley, T. Shibauchi, L. Krusin-Elbaum, K. Guarini, C.T. Black, M.T. Tuominen, T.P. Russell, Science 290 (2000) 2126.
[5] P.N. Bartlett, P.R. Birkin, M.A. Ghanem, Chem. Commun. (2000) 1671.

[6] L. Xu, W.L. Zhou, C. Frommen, R.H. Baughman, A.A. Zakhidov, L. Malkinski, J.Q. Wang, J.B. Wiley, Chem. Commun. (2000) 997.

[7] D. Wang, H. Mohwald, J. Mater. Chem. 14 (2004) 459.

[8] P. Ferrand, M. Egen, B. Griesebock, J. Ahopelto, M. Muller, R. Zentel, S.G. Romanov, C.M. Sotomayor, Appl. Phys. Lett. 81 (2002) 2689.

[9] J.P. Hoogenboom, C. Retif, E. de Bres, M. van de Boer, A.K. van Langen-Suurling, J. Romijn, A. van Blaaderen, Nanoletters 4 (2004) 205.

[10] J.C. Cheng, A.M. Mayes, C.A. Boss, Nat. Mater. 3 (2004) 823.

[11] M.E. Kiziroglou, A.A. Zhukov, X. Li, D.C. Gonzalez, P.A.J. de Groot, P.N. Bartlett, C.H. de Groot, J. Appl. Phys. 10 (2006) 113720.

[12] S.M. Weekes, F.Y. Ogrin, W.A. Murray, Langmuir 20 (2004) 11208.

[13] M. Albrecht, G. Hu, I.L. Guhr, T.C. Ulbrich, J. Boneberg, P. Leiderer, G. Schatz, Nat. Mater. 4 (2005) 203.

[14] A.A. Zhukov, M.E. Kiziroglou, A.V. Goncharov, R. Boardman, M.A. Ghanem, M. Abdelsalam, V. Novosad, G. Karapetrov, X. Li, H. Fangohr, C.H. de Groot, P.N. Bartlett, P.A.J. de Groot, IEEE Trans. Magn. 41 (2005) 3598.

[15] M.E. Kiziroglou, A.A. Zhukov, M. Abdelsalam, X. Li, P.A.J. de Groot, P.N. Bartlett, C.H. de Groot, IEEE Trans. Magn. 41 (2005) 2639.

[16] Object Oriented MicroMagnetic Framework [Online]. Available: ⟨http://math.nist.gov/oommf/⟩.

[17] D. Craik, Magnetism Principles and Applications, Wiley, 1995, p. 404. H. Kronmüller, M. Fähnle, Micromagnetism and the Microstructure of Ferromagnetic Solids, first ed., Cambridge, 2003, pp. 17–22.